were observed among genotyping groups of *ABCG2*. To ensure the quality of the study, we selected *SLCO1B1* and *ABCG2* genotyping-matched volunteers from our panels. However, unfortunately, as the frequency of the *SLCO1B1*15/*15* is low in Japanese populations,[15] we recruited one miss-matched 421C/A subject in group 3 (*i.e.*, *15/*15), which could have consequences for the interpretation of the results.

In this study, the mean AUC_{0-24} and C_{max} values in homozygotes for the *SLCO1B1*15* allele were 3.1- and 4.1-fold higher, respectively, than those in *SLCO1B1*1b/*1b* subjects, and heterozygotes had values between the two homozygous groups. These findings were consistent with a recent study conducted by Chung *et al.*[18] Although no homozygotes for the *15 allele were included in their study, they found dose-normalized AUC and C_{max} of pitavastatin to be 1.4- and 1.8-fold higher, respectively, in subjects heterozygous for the *15 allele versus subjects without this allele. Several transporters are known to be involved in the hepatic uptake of clinically important drugs in humans. Among them, a recent *in vitro* study indicated that the uptake clearance of pitavastatin in human hepatocytes could be almost completely accounted for by OATP1B1 and OATP1B3 (OATP8), but approximately 90% of the total hepatic clearance could be accounted for by OATP1B1.[6] Thus, similar to pravastatin, OATP1B1 is suggested to play an important role in the hepatic uptake of pitavastatin in humans.

The 174Val > Ala variant has been consistently associated with reduced transport activity of OATP1B1 both *in vitro*[14,31] and *in vivo*.[15–18] As selective distribution to the liver may also be the first step for the pharmacological action of pitavastatin, subjects with this variant (*i.e.*, *5, *15, and *17 alleles) are expected to exhibit a reduced cholesterol-lowering effect owing to the lower pitavastatin concentration in hepatocytes, despite high plasma concentrations and AUC of pitavastatin. To date, some groups have reported the implication of the *SLCO1B1* polymorphism in the lipid-lowering efficacy of statins under multiple-dose conditions[32] and chronic treatment.[33–35] Igel *et al.*[32] conducted a healthy volunteer study ($n = 16$) and demonstrated no significant difference in the lipid-lowering efficacy of pravastatin between the variant allele (*15 and *17 alleles) and control groups after treatment with 40 mg pravastatin daily for 3 weeks, despite considerably higher plasma pravastatin concentration in the variant group. Similarly, in a study of 33 patients with hypercholesterolemia treated with pravastatin (mean dose of 9.4 mg/day), the genotype-dependent difference in the lipid-lowering effect in the initial phase of treatment (8 weeks) disappeared after 1 year of treatment.[33] In addition to experimental designs, such as the male/female ratio[36] and racial background, numerous genetic factors may have an impact on the response to statins.[32,37] Furthermore, the 174Val > Ala variant is associated with reduced transport activity, but does not lead to loss of activity,[14,31] making it conceivable that there is no significant impact of the genotype on the clinical efficacy of statins during long-term treatment; however, a high plasma concentration, on the other hand, is known as a risk factor for the myotoxic effects of statins.[38] The effect of the polymorphism of the *SLCO1B1* gene on the clinical efficacy and adverse events of pitavastatin will be the subject of further investigation.

In this study, the AUC_{0-24} of the lactone form was comparable with that of the acid form, and the pharmacokinetics of lactone was not affected by the *SLCO1B1* polymorphism. The profile of the hepatic uptake of lactone has not yet been elucidated; however, our study indicated that OATP1B1 can be ruled out as a candidate transporter in humans. As the lactone form can be reversibly converted to the acid form in the body, it can be asked whether a comparably high serum concentration of lactone contributes to the clinical efficacy of pitavastatin. In the acid/lactone interconversion of pitavastatin, the following pathways have been proposed: the first step is the glucuronidation of pitavastatin to form UM-2 as an intermediate to the lactone form by uridine 5′-diphosphate glucuronosyl transferases (UGT1A1, 1A3, and 2B7). The glucuronic acid moiety is subsequently converted nonenzymatically to its lactone form. After conversion, some of the resulting lactone form changes to the acid form by hydrolysis. Cytochrome p450 3A4-mediated metabolism of the lactone form was also observed in human hepatic microsomes.[3,4] Furthermore, in addition to the liver, lactone may form in extrahepatic tissues such as the kidney and intestine.[4] Although the metabolism of pitavastatin is complex, lactonization is the major metabolic pathway in humans.[4] These findings suggest that a certain amount of pitavastatin acid produced from the lactone form by hepatic interconversion has a clinical impact on the lipid-lowering effect. Further study with regard to the *SLCO1B1* polymorphism, in which the pitavastatin lactone form is used as a test drug, is required.

In addition to AUC_{0-24}, the mean C_{max} was higher in subjects with the *15 allele than in subjects without this allele. To discuss this point, we estimated the pharmacokinetic data using WinNonlin. Although the difference did not reach the level of significance, V_d/F values tended to be lower in subjects with the *15 allele (**Table 1**). The V_d of pitavastatin in the liver ($V_{d_{liver}}$) can be estimated by the following equation: $K_{P_{liver}} \times V_{liver}$, where $K_{P_{liver}}$ is the $C_{P_{liver}}/C_{P_{plasma}}$ ratio (approximately 23.0 in rats),[9] and V_{liver} is the liver volume (approximately 78.4 ml/kg).[39] Estimated $V_{d_{liver}}$ (1.8 l/kg) and V_d/F (1.0 l/kg)[9] are comparable, suggesting that the liver is the major organ for the distribution of pitavastatin in rats. In addition, total clearance of pitavastatin (0.15–0.43 l/h/kg in this study) is relatively lower than that of other statins in humans (800–1000 l/h for simvastatin,[40] 0.8–2.7 l/h/kg for pravastatin,[15] 80–200 l/h for rosuvastatin,[41] and 150–1200 l/h for atorvastatin[42]). Taking these *in vivo* findings into consideration, a decreased V_d of pitavastatin owing to low transport activity is one of the possible reasons for high C_{max} values in subjects with the *15 allele. Nevertheless, changes in F cannot be denied in such subjects because there is no

intravenous data for pitavastatin to determine absolute value of bioavailability.

In this study, no change in K_e values was observed. Although a firm conclusion cannot be reached regarding possible changes in V_d versus F (again, because of no intravenous data), *OATP1B1*15* allele may be associated with decreased CL_r and V_d values simultaneously, which may cancel out the change in K_e values.

It was somewhat unexpected that there were no significant differences in any pharmacokinetic parameters among *ABCG2* (421C>A) genotypic groups because some *in vivo* studies demonstrated that the 421C>A allele was associated with changes in the pharmacokinetics of certain clinically important substrate drugs, such as diflomotecan[26] and topotecan.[43] In addition, Zhang *et al.*[29] recently studied rosuvastatin pharmacokinetics in relation to the *ABCG2* 421C>A polymorphism in 14 healthy volunteers. Although they used an insufficient number of subjects, they demonstrated that the AUC of rosuvastatin was lower in subjects with the 421C/C genotype than in subjects with 421A variant(s). Available data indicate that the 421C>A variant was associated with remarkably decreased BCRP expression compared with wild-type cells and human placental samples,[22,27] which may lead to the following changes based on its localization; increased absorption at the intestinal epithelium, and/or decreased biliary excretion of substrates, thereby resulting in elevated plasma concentrations in subjects with 421A variant(s). Although both pitavastatin and rosuvastatin seem to be good substrates for BCRP,[9,44] our present findings were clearly in contrast to the findings reported by Zhang *et al.*[29] This discrepancy may be explained as follows: a recent *in vitro* experiment using double-transfected Madin-Darby cainine kidney (MDCK) II monolayers expressing OATP1B1 and human canalicular efflux transporters indicated that the significant transport of pitavastatin was observed in OATP1B1/MDR1 and OATP1B1/MRP2 as well as OATP1B1/BCRP double transfectants.[9] These results suggest that multiple organic anion transporters across the canalicular membrane in the liver are involved in the biliary excretion of pitavastatin.

Hirano *et al.*[9] have previously shown that the biliary excretion of pitavastatin in Bcrp1 (−/−) mice was drastically reduced compared with that in control mice after constant infusion, although the steady-state plasma concentration in Bcrp1 (−/−) mice is not different from that in control mice owing to the extensive metabolism of pitavastatin in mice. As BCRP is also expressed on the brush-border membrane of enterocytes, reduced function because of modulation of the expression level or recognition/affinity capability may lead to the increasing intestinal absorption of substrate drugs; therefore, we compared the pharmacokinetics of pitavastatin after oral administration in Bcrp1 (−/−) and control mice. Similar to the constant infusion, the time profiles of the plasma concentration of pitavastatin were not different between Bcrp1 (−/−) and control mice (**Figure 3**). These results suggest that, in contrast to the biliary excretion, Bcrp1 is not important as a determinant of intestinal absorption. In our animal study, the dose of pitavastatin was considerably higher and also the plasma concentrations appeared to be somewhat higher in mice than those observed in our subjects. In addition to these experimental designs, the metabolic profile of pitavastatin is reported to be different between mice and men;[9] however, our present findings suggest that the contribution of BCRP to the pharmacokinetics of pitavastatin is not significant as our expectations in humans.

Although all statins share a common action mechanism, they differ in terms of their chemical structures, pharmacokinetics, and pharmacodynamics. In particular, transporters involved in biliary excretion are different among statins; for example, ABCC2 (MRP2) is reported to be responsible for pravastatin both *in vitro* and *in vivo*.[9,45,46] In addition to efflux, a recent study indicated that multiple transporters are involved in the hepatic uptake of statins.[47] These differences make the understanding of the transport mechanism of statins difficult. Differences in the pharmacokinetic profiles between acid and lactone forms of pitavastatin observed in this study can be partially attributed to the contribution of multiple transporters.[48] However, hepatic uptake of pravastatin and pitavastatin, and probably rosuvastatin,[41] by OATP1B1 seems to be the major determinant of their overall pharmacokinetic profiles (*i.e.*, elimination and tissue distribution) in humans. Indeed, numerous OATP1B1-mediated drug–drug interactions have been reported to date, suggesting that transporter-mediated hepatic uptake is the main determinant of plasma clearance, even for drugs undergoing extensive metabolism.[49]

METHODS

Subjects and genotyping of *SLCO1B1* and *ABCG2*. After approval by the Ethics Review Board of Kyushu University and Kyushu Clinical Pharmacology Research Clinic, 38 healthy male volunteers (age, 20–32 years; weight, 52.4–72.4 kg) gave written informed consent to participate in the study. None had taken any drugs for at least 1 week before the study. Each subject was physically normal and had no antecedent history of significant medical illness or hypersensitivity to any drugs, and each had a body mass index between 17.6 and 26.4 kg/m^2. Their health status was judged to be normal on the basis of a physical examination with screening of blood chemistry, a complete blood count and urinalysis, and an electrocardiogram just before the study.

The genotyping methods of *SLCO1B1* and *ABCG2* have been described previously.[15,22] Single-strand conformation polymorphism and polymerase chain reaction–restriction fragment length polymorphism methods were used for genotyping. In this study, *1b and *15 alleles and 421C>A variant were identified for *SLCO1B1* and *ABCG2* genes, respectively, and all subjects were divided into the following groups: 421C/C*1b/*1b (group 1, $n=11$), 421C/C*1b/*15 (group 2, $n=8$), 421C/C*15/*15 ($n=2$) and 421C/A*15/*15 ($n=1$) (group 3), 421C/A*1b/*1b (group 4, $n=7$), 421A/A*1b/*1b (group 5, $n=3$), and 421C/A*1b/*15 (group 6, $n=6$).

Study protocol. The participants came to the clinic after an overnight fast. They were required to abstain from alcohol for 2 days before drug administration and during the period of hospitalization and were served standard meals on the study day. Each volunteer received a single oral dose of 2 mg of pitavastatin (Livalo, Kowa,

Nagoya, Japan) with 150 ml of water. Venous blood samples (7 ml each) to determine pitavastatin and pitavastatin lactone concentrations were obtained just before and 0.5, 1, 1.5, 2, 4, 6, 8, 12, and 24 h after dosing. Plasma samples were immediately separated after centrifugation and stored at −70°C until analyzed.

Quantification of pitavastatin and pitavastatin lactone in plasma. The concentrations of pitavastatin and its lactone in plasma were measured by high-performance liquid chromatography (HPLC) according to the methods of Kojima *et al.*[50] with a minor modification. The plasma sample (1.0 ml) was mixed with 0.2 ml internal standard (I-1938, 125 ng/ml; supplied by Nissan Chemical Industries (Saitama, Japan)), 0.2 ml water, 10 μl acetonitrile, and 0.5 ml 1.0 M potassium dihydrogenphosphate in a colored tube. The sample mixture was extracted with 8 ml of methyl *tert*-butyl ether by shaking for 10 min on a horizontal shaker at 200 r.p.m. and by centrifuging for 10 min at approximately 1,720 × *g* (at 4°C). The organic layer was transferred to another colored tube and subsequently diazomethane-diethyl ether solution (0.5 ml) was added. The reaction mixture was kept at room temperature for 30 min. To degrade excessive diazomethane, 1.0 M potassium dihydrogenphosphate (2 ml) was added to the mixture. After centrifuging for 10 min at 1,720 × *g*, the organic layer was evaporated to dryness under a gentle stream of nitrogen at 40°C. The residue was reconstituted in 150 μl of mobile phase for pre-separation and an aliquot of 80 μl was injected into the HPLC system. Column-switching HPLC (using a six-port switching valve) was performed with two Cosmosil-C18-MS-II columns (150 × 4.6 mm internal diameter; Nacalai Tesque, Kyoto, Japan) for pre-separation and analytical separation. Two mobile phases, 0.2 M ammonium acetate buffer (pH 4.0)–acetonitrile (5:5, v/v) for pre-separation and 0.2 M acetic acid–acetonitrile (5:5, v/v) for analytical separation, were maintained at a flow rate of 1.0 ml/min. Detection was carried out at 250 nm with a UV detector. Column temperature was maintained at 40°C. Calibration curves for both analytes ranged from 0.5 to 200 ng/ml. This HPLC method was validated only for the measurement of serum concentrations of pitavastatin and lactone in the human study. The intraday coefficient of variation values were less than 13.0% and intraday accuracies were between −14.0 and 6.0%, within the concentration range of the calibration curves for both analytes. Interday coefficient of variation values were less than 5.0% and interday accuracies were between −2.4 and 4.7%. The limits of quantification for both analytes were set to 0.5 ng/ml.[50]

***In vivo* study in mice and quantification of pitavastatin by liquid chromatography/mass spectrometry.** Male FVB control and Bcrp1 (−/−) mice weighing approximately 28–33 g were used throughout these experiments. Pitavastatin was orally administered to both mice at a dose of 10 mg/kg. Blood samples were collected from the tail vein at 0.5, 1, 2, 3, and 4 h after oral administration of pitavastatin. The plasma sample (10 μl) was mixed with 100 μl methanol containing the internal standard (atorvastatin, 80 ng/ml), followed by centrifugation (10,000 × *g*) at 4°C for 10 min. Atorvastatin was synthesized by Kowa (Tokyo, Japan). The supernatant (80 μl) was mixed with 50 μl water and subjected to HPLC (Waters 2695; Waters, Milford, MA). Liquid chromatography/mass spectrometry analysis of pitavastatin was performed with an Inertsil ODS-3 column (50 × 2.1 mm internal diameter, particle size 5 μm) (GL Sciences, Tokyo, Japan). The mobile phase consisted of methanol–ammonium formate buffer (pH 4.0, 7:3, v/v) and the flow rate was 0.5 ml/min. The mass spectrometry instrument used for this work was a ZQ micro-mass (Waters) equipped with a Z-spray source and operated in the positive-ion electrospray ionization mode. The Z-spray desolvation temperature, capillary voltage, and cone voltage were 350°C, 3400 V and 40 V, respectively. The *m/z* monitored for pitavastatin and atorvastatin was 422.3 and 559.0, respectively. No chromatographic interference was found for pitavastatin and atorvastatin in extracts from blank plasma. The retention times of pitavastatin and atorvastatin were 1.5 and 1.4 min, respectively. The calibration curves for pitavastatin ranged from 5 to 1000 ng/ml. This liquid chromatography/mass spectrometry method was validated only for the measurement of serum concentration of pitavastatin in the animal study. For pitavastatin, quality control samples covering the whole concentration range showed high intra- and interday accuracy and reproducibility with a coefficient of variation and bias below 10%.

Pharmacokinetics and statistical analysis. C_{max} was obtained directly from the data. AUC_{0-24} was calculated by the linear trapezoidal rule. We calculated the CL_t of pitavastatin as follows: $CL_t = Dose/AUC_{0-24}$. The K_e was estimated using least-squares regression analysis from the terminal postdistribution phase of the concentration–time curve. To assess differences in the V_d/F of pitavastatin in relation to the *SLCO1B1* polymorphism, we also estimated model-dependent parameters (one-compartment open model with first-order elimination and no lag time) using the WinNonlin 5.0.1 program (Pharsight, Mountain View, CA). Statistical differences among the data for each group were determined by analysis of variance, followed by Fisher's least significant difference test. $P < 0.05$ was considered statistically significant.

ACKNOWLEDGMENTS

This study was supported by a Health and Labour Sciences Research Grant from the Ministry of Health, Labour and Welfare for Research on Advanced Medical Technology.

CONFLICT OF INTEREST

The authors declared no conflict of interest.

1. Aoki, T. *et al.* Pharmacological profile of a novel synthetic inhibitor of 3-hydroxy-3-methylglutaryl-coenzyme A reductase. *Arzneimittelforschung* **47,** 904–909 1997.
2. Fujino, H., Yamada, I., Shimada, S., Nagao, T. & Yoneda, M. Metabolic fate of pitavastatin (NK-104), a new inhibitor of 3-hydroxy-3-methyl-glutaryl coenzyme A reductase. Effects on drug-metabolizing systems in rats and humans. *Arzneimittelforschung* **52,** 745–753 2002.
3. Fujino, H., Saito, T., Tsunenari, Y., Kojima, J. & Sakaeda, T. Metabolic properties of the acid and lactone forms of HMG-CoA reductase inhibitors. *Xenobiotica* **34,** 961–971 2004.
4. Fujino, H., Yamada, I., Shimada, S., Yoneda, M. & Kojima, J. Metabolic fate of pitavastatin, a new inhibitor of HMG-CoA reductase: human UDP-glucuronosyltransferase enzymes involved in lactonization. *Xenobiotica* **33,** 27–41 2003.
5. Yamada, I., Fujino, H., Shimada, S. & Kojima, J. Metabolic fate of pitavastatin, a new inhibitor of HMG-CoA reductase: similarities and difference in the metabolism of pitavastatin in monkeys and humans. *Xenobiotica* **33,** 789–803 2003.
6. Hirano, M., Maeda, K., Shitara, Y. & Sugiyama, Y. Contribution of OATP2 (OATP1B1) and OATP8 (OATP1B3) to the hepatic uptake of pitavastatin in humans. *J. Pharmacol. Exp. Ther.* **311,** 139–146 2004.
7. Hagenbuch, B. & Meier, P.J. The superfamily of organic anion transporting polypeptides. *Biochim. Biophys. Acta* **1609,** 1–18 2003.
8. Hsiang, B. *et al.* A novel human hepatic organic anion transporting polypeptide (OATP2). Identification of a liver-specific human organic anion transporting polypeptide and identification of rat and human hydroxymethylglutaryl-CoA reductase inhibitor transporters. *J. Biol. Chem.* **274,** 37161–37168 1999.
9. Hirano, M., Maeda, K., Matsushima, S., Nozaki, Y., Kusuhara, H. & Sugiyama, Y. Involvement of BCRP (ABCG2) in the biliary excretion of pitavastatin. *Mol. Pharmacol.* **68,** 800–807 2005.
10. Cervenak, J. *et al.* The role of the human ABCG2 multidrug transporter and its variants in cancer therapy and toxicology. *Cancer Lett.* **234,** 62–72 2006.

11. Maliepaard, M. *et al.* Subcellular localization and distribution of the breast cancer resistance protein transporter in normal human tissues. *Cancer Res.* **61,** 3458–3464 2001.
12. Kruijtzer, C.M., Beijnen, J.H. & Schellens, J.H. Improvement of oral drug treatment by temporary inhibition of drug transporters and/or cytochrome P450 in the gastrointestinal tract and liver: an overview. *Oncologist* **7,** 516–530 2002.
13. Taipalensuu, J. *et al.* Correlation of gene expression of ten drug efflux proteins of the ATP-binding cassette transporter family in normal human jejunum and in human intestinal epithelial Caco-2 cell monolayers. *J. Pharmacol. Exp. Ther.* **299,** 164–170 2001.
14. Tirona, R.G., Leake, B.F., Merino, G. & Kim, R.B. Polymorphisms in OATP-C: identification of multiple allelic variants associated with altered transport activity among European- and African-Americans. *J. Biol. Chem.* **276,** 35669–35675 2001.
15. Nishizato, Y. *et al.* Polymorphisms of OATP-C (SLC21A6) and OAT3 (SLC22A8) genes: consequences for pravastatin pharmacokinetics. *Clin. Pharmacol. Ther.* **73,** 554–565 2003.
16. Niemi, M. *et al.* High plasma pravastatin concentrations are associated with single nucleotide polymorphisms and haplotypes of organic anion transporting polypeptide-C (OATP-C SLCO1B1). *Pharmacogenetics* **14,** 429–440 2004.
17. Mwinyi, J., Johne, A., Bauer, S., Roots, I. & Gerloff, T. Evidence for inverse effects of OATP-C (SLC21A6) 5 and 1b haplotypes on pravastatin kinetics. *Clin. Pharmacol. Ther.* **75,** 415–421 2004.
18. Chung, J.Y. *et al.* Effect of OATP1B1 (SLCO1B1) variant alleles on the pharmacokinetics of pitavastatin in healthy volunteers. *Clin. Pharmacol. Ther.* **78,** 342–350 2005.
19. Niemi, M., Kivisto, K.T., Hofmann, U., Schwab, M., Eichelbaum, M. & Fromm, M.F. Fexofenadine pharmacokinetics are associated with a polymorphism of the SLCO1B1 gene (encoding OATP1B1). *Br. J. Clin. Pharmacol.* **59,** 602–604 2005.
20. Niemi, M. *et al.* Polymorphic organic anion transporting polypeptide 1B1 is a major determinant of repaglinide pharmacokinetics. *Clin. Pharmacol. Ther.* **77,** 468–478 2005.
21. Maeda, K. *et al.* Effects of organic anion transporting polypeptide 1B1 haplotype on pharmacokinetics of pravastatin, valsartan, and temocapril. *Clin. Pharmacol. Ther.* **79,** 427–439 2006.
22. Kobayashi, D. *et al.* Functional assessment of ABCG2 (BCRP) gene polymorphisms to protein expression in human placenta. *Drug Metab. Dispos.* **33,** 94–101 2005.
23. Iida, A. *et al.* Catalog of 605 single-nucleotide polymorphisms (SNPs) among 13 genes encoding human ATP-binding cassette transporters: ABCA4, ABCA7, ABCA8, ABCD1, ABCD3, ABCD4, ABCE1, ABCF1, ABCG1, ABCG2, ABCG4, ABCG5, and ABCG8. *J. Hum. Genet.* **47,** 285–310 2002.
24. Zamber, C.P. *et al.* Natural allelic variants of breast cancer resistance protein (BCRP) and their relationship to BCRP expression in human intestine. *Pharmacogenetics* **13,** 19–28 2003.
25. Backstrom, G. *et al.* Genetic variation in the ATP-binding cassette transporter gene ABCG2 (BCRP) in a Swedish population. *Eur. J. Pharm. Sci.* **18,** 359–364 2003.
26. Sparreboom, A. *et al.* Diflomotecan pharmacokinetics in relation to ABCG2 421C > A genotype. *Clin. Pharmacol. Ther.* **76,** 38–44 2004.
27. Kondo, C. *et al.* Functional analysis of SNPs variants of BCRP/ABCG2. *Pharm. Res.* **21,** 1895–1903 2004.
28. Imai, Y. *et al.* C421A polymorphism in the human breast cancer resistance protein gene is associated with low expression of Q141K protein and low-level drug resistance. *Mol. Cancer Ther.* **1,** 611–616 2002.
29. Zhang, W. *et al.* Role of BCRP 421C > A polymorphism on rosuvastatin pharmacokinetics in healthy Chinese males. *Clin. Chim. Acta* **373,** 99–103 2006.
30. Schachter, M. Chemical, pharmacokinetic and pharmacodynamic properties of statins: an update. *Fundam. Clin. Pharmacol.* **19,** 117–125 2005.
31. Kameyama, Y., Yamashita, K., Kobayashi, K., Hosokawa, M. & Chiba, K. Functional characterization of SLCO1B1 (OATP-C) variants, SLCO1B1*5, SLCO1B1*15 and SLCO1B1*15+C1007G, by using transient expression systems of HeLa and HEK293 cells. *Pharmacogenet. Genomics* **15,** 513–522 2005.
32. Igel, M. *et al.* Impact of the SLCO1B1 polymorphism on the pharmacokinetics and lipid-lowering efficacy of multiple-dose pravastatin. *Clin. Pharmacol. Ther.* **79,** 419–426 2006.
33. Takane, H. *et al.* Pharmacogenetic determinants of variability in lipid-lowering response to pravastatin therapy. *J. Hum. Genet.* **51,** 822–826 2006.
34. Tachibana-Iimori, R. *et al.* Effect of genetic polymorphism of OATP-C (SLCO1B1) on lipid-lowering response to HMG-CoA reductase inhibitors. *Drug Metab. Pharmacokinet.* **19,** 375–380 2004.
35. Thompson, J.F. *et al.* An association study of 43 SNPs in 16 candidate genes with atorvastatin response. *Pharmacogenomics J.* **5,** 352–358 2005.
36. Niemi, M., Pasanen, M.K. & Neuvonen, P.J. SLCO1B1 polymorphism and sex affect the pharmacokinetics of pravastatin but not fluvastatin. *Clin. Pharmacol. Ther.* **80,** 356–366 2006.
37. Chasman, D.I., Posada, D., Subrahmanyan, L., Cook, N.R., Stanton, V.P. Jr. & Ridker, P.M. Pharmacogenetic study of statin therapy and cholesterol reduction. *JAMA* **291,** 2821–2827 2004.
38. Thompson, P.D., Clarkson, P. & Karas, R.H. Statin-associated myopathy. *JAMA* **289,** 1681–1690 2003.
39. Davies, B. & Morris, T. Physiological parameters in laboratory animals and humans. *Pharm. Res.* **10,** 1093–1095 1993.
40. Pasanen, M.K., Neuvonen, M., Neuvonen, P.J. & Niemi, M. SLCO1B1 polymorphism markedly affects the pharmacokinetics of simvastatin acid. *Pharmacogenet. Genomics* **16,** 873–879 2006.
41. Lee, E. *et al.* Rosuvastatin pharmacokinetics and pharmacogenetics in white and Asian subjects residing in the same environment. *Clin. Pharmacol. Ther.* **78,** 330–341 2005.
42. Hermann, M. *et al.* Exposure of atorvastatin is unchanged but lactone and acid metabolites are increased several-fold in patients with atorvastatin-induced myopathy. *Clin. Pharmacol. Ther.* **79,** 532–539 2006.
43. Sparreboom, A. *et al.* Effect of ABCG2 genotype on the oral bioavailability of topotecan. *Cancer Biol. Ther.* **4,** 650–658 2005.
44. Huang, L., Wang, Y. & Grimm, S. ATP-dependent transport of rosuvastatin in membrane vesicles expressing breast cancer resistance protein. *Drug Metab. Dispos.* **34,** 738–742 2006.
45. Kivisto, K.T. *et al.* Disposition of oral and intravenous pravastatin in MRP2-deficient TR-rats. *Drug Metab. Dispos.* **33,** 1593–1596 2005.
46. Niemi, M. *et al.* Association of genetic polymorphism in ABCC2 with hepatic multidrug resistance-associated protein 2 expression and pravastatin pharmacokinetics. *Pharmacogenet. Genomics* **16,** 801–808 2006.
47. Ho, R.H. *et al.* Drug and bile acid transporters in rosuvastatin hepatic uptake: function, expression, and pharmacogenetics. *Gastroenterology* **130,** 1793–1806 2006.
48. Fujino, H., Saito, T., Ogawa, S. & Kojima, J. Transporter-mediated influx and efflux mechanisms of pitavastatin, a new inhibitor of HMG-CoA reductase. *J. Pharm. Pharmacol.* **57,** 1305–1311 2005.
49. Shitara, Y. & Sugiyama, Y. Pharmacokinetic and pharmacodynamic alterations of 3-hydroxy-3-methylglutaryl coenzyme A (HMG-CoA) reductase inhibitors: drug-drug interactions and interindividual differences in transporter and metabolic enzyme functions. *Pharmacol. Ther.* **112,** 71–105 2006.
50. Kojima, J., Fujino, H., Yosimura, M., Morikawa, H. & Kimata, H. Simultaneous determination of NK-104 and its lactone in biological samples by column-switching high-performance liquid chromatography with ultraviolet detection. *J. Chromatogr. B. Biomed. Sci. Appl.* **724,** 173–180 1999.

CHAPTER

Single nucleotide polymorphism typing using degenerate-oligonucleotide-primed PCR-amplified products

Makoto Bannai[1] and Katsushi Tokunaga[2]

[1]Biomedical Business R&D Department, Olympus Corporation, 2-3 Kuboyama-cho, Hachioji-shi, Tokyo 192-8512, Japan; [2]Department of Human Genetics, Graduate School of Medicine, The University of Tokyo, 7-3-1 Hongo, Bunkyo-ku, Tokyo 113-0033, Japan

1. INTRODUCTION

WGA is a valuable technique for amplifying a limited amount of DNA in a sequence-independent fashion. WGA methods have been adopted for minimization of the amount of genomic DNA needed for a number of biological assays including large-scale typing of single nucleotide polymorphisms (SNPs), microsatellite genotyping, and comparative genomic hybridization (CGH).

WGA by degenerate-oligonucleotide-primed PCR (DOP-PCR) was first described by Telenius *et al.* (1) and allows complete genome coverage in a single reaction. In contrast to the pairs of target-specific primer sequences used in traditional PCR, only a single primer, which has defined sequences at its 5′ (containing a *Xho*I restriction site, highlighted in bold) and 3′ ends and a random hexamer sequence between them (5′-CCGA**CTCGAG**NNNNNNATGTGG-3′), is used for DOP-PCR. Compared with completely degenerate primers, such as those used for primer-extension pre-amplification PCR (PEP-PCR) (5′-NNNNNNNNNNNNNN-3′), the primer for DOP-PCR is relatively specific (2).

DOP-PCR is comprised of two different cycling stages, low stringency and high stringency. At low stringency, the 3′ end of the primer binds at sites in the genome complementary to the 6 bp well-defined sequence (approximately 10^6 sites in the human genome). The adjacent random hexamer sequence, which displays all possible combinations of the nucleotides A, G, C, and T, then enables efficient primer annealing and the start of the DOP-PCR-based WGA reaction.

Whole Genome Amplification: *Methods Express* (S. Hughes and R. Lasken, eds.)

Since its conception, several modifications of the basic DOP-PCR protocol have been devised with the purpose of lowering the required amount of starting template (3) and increasing yield (4), fidelity, and fragment length (5), in order to provide better coverage of the genome. However, all have used the same basic methodology.

2. METHODS AND APPROACHES

2.1. Methodology of DOP-PCR

Within a single PCR tube, low-temperature annealing and extension in the first five to eight cycles of DOP-PCR occurs at many binding sites in the genome (see *Fig. 1a* and *Protocol 2*, Stage 1 - low stringency) and tags these sequences with the DOP primer. Thereafter, the annealing temperature of the PCR (>25 cycles) is increased to allow more specific priming and amplification of the tagged sequence (see *Fig. 1a* and *Protocol* 2, Stage 2 - high stringency). DOP-PCR amplification ideally results in a smear of DNA fragments (200–1000 bp) that are visible on an agarose gel stained with ethidium bromide (see *Fig. 1b*).

2.2. Applications of DOP-PCR

DOP-PCR is often used as the first step in *in situ* hybridization for flow-sorted (1, 6) or microdissected (7) chromosomes and for CGH (7, 8). This approach has been successfully modified and applied to genomic DNA for genotyping of microsatellites (9) and for typing of SNPs (10–12). In this chapter, we describe sequence-specific primer PCR (SSP-PCR) followed by fluorescence correlation spectroscopy (FCS) as a method for applying DOP-PCR to SNP typing (11).

3. RECOMMENDED PROTOCOLS

Although we have named specific suppliers for the reagents and equipment used in this chapter, other manufacturers' products are likely to generate similar results. However, it is up to the user to test this.

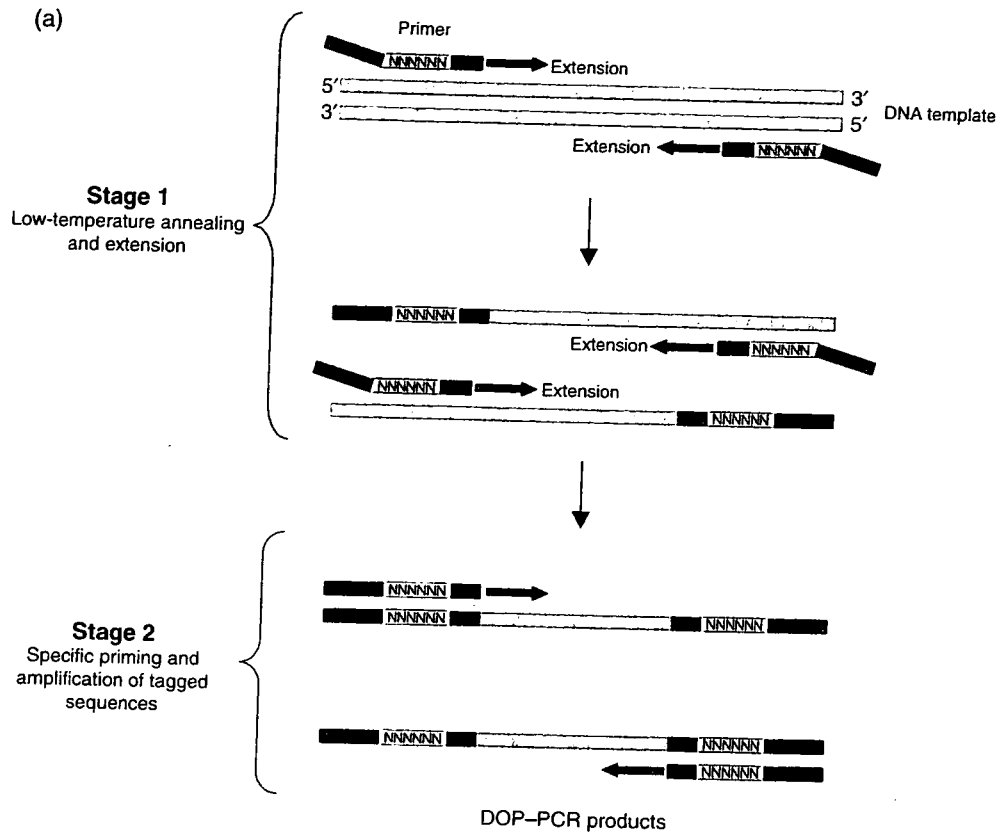

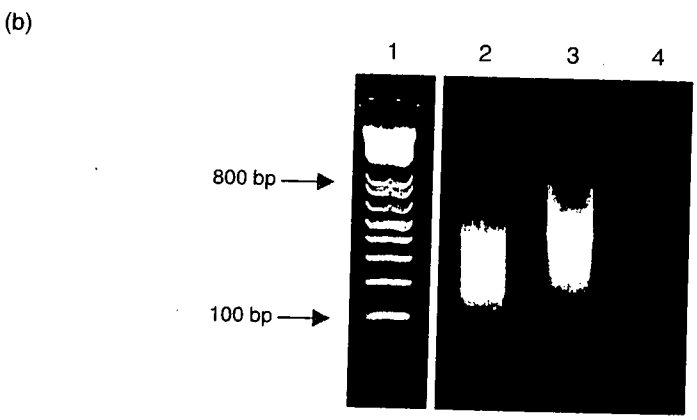

Figure 1. DOP–PCR.
(*a*) Graphical representation of the steps involved in DOP–PCR. Low-temperature annealing and extension in the first five to eight cycles of DOP–PCR occurs at many binding sites in the genome (Stage 1) and tags these sequences with the DOP primer. Thereafter, the annealing temperature of the PCR (>25 cycles) is increased to allow more specific priming and amplification of the tagged sequence (Stage 2). (*b*) Agarose gel stained with ethidium bromide displaying the smear of DNA fragments typically obtained from DOP–PCR WGA. (*Lane 1*) 100 bp ladder; (*lane 2*) DOP–PCR product obtained from DNA extracted from formalin-fixed, paraffin-embedded tissue; (*lane 3*) DOP–PCR product obtained from DNA extracted from fresh tissue; (*lane 4*) negative control.

Protocol 1

Genomic DNA extraction and quantification

Equipment and Reagents

- QIAamp DNA Blood Midi Kit (Qiagen)
- PicoGreen dsDNA quantitation reagent (Molecular Probes)
- 10 mM Tris-HCl (pH 8.0) containing 0.1 mM EDTA
- Fluorescence-based microplate reader

Method

1. Isolate genomic DNA from peripheral blood using the QIAamp DNA Blood Midi Kit according to the manufacturer's instructions.
2. Measure the genomic DNA concentration using the PicoGreen dsDNA quantitation reagent according to the manufacturer's instructions.
3. Dilute the DNA samples to 10 ng/μl with 10 mM Tris-HCl (pH 8.0) containing 0.1 mM EDTA.

DNA yields of approximately 4–6 μg are typically obtained in a 100 μl reaction. The diluted DOP-PCR product (approximately 10–15 ng/μl) can be used as template in a subsequent PCR to generate fragments including SNP sites. The PCR products can then be sequenced.

SSP-PCR followed by FCS is applied for high-throughput SNP typing and has been described previously (11). The first PCR is followed by SSP-PCR using the product from the first PCR as template. Allele-specific, semi-nested primers are used for the SSP-PCR. They differ in a single nucleotide at the 3′ end and are coupled to different fluorescence dyes – 6-carboxytetramethylrhodamine (TAMRA) or cyanine 5 (Cy5). Because the movement of DNA fragments in a solution depends on their size, primers (smaller molecules) move faster than SSP-PCR-amplified fragments (larger molecules) in the PCR product solution. When the narrow laser beam spots DNA fragments in the solution (in a 1 fl volume), the signals from the fluorescent-labeled molecules are detected by a highly sensitive spectrophotometer, allowing determination of the numbers and sizes of both primers and amplified fragments. The percentage of allele-specific amplified fragments relative to the total number of fluorescent-labeled molecules can then be determined using the single-molecule fluorescence detection system.

Protocol 2

DOP-PCR[a]

Equipment and Reagents

- 4 µM DOP primer (5′-CCGACTCGAGNNNNNNATGTGG-3′) (Sigma Genosys)
- TaKaRa LA *Taq* polymerase (5 units/µl) and accompanying 2× GC buffer (Takara Bio)
- 400 µM dNTP mix (Takara Bio)
- Nuclease-free water (Sigma)
- 10 mM Tris-HCl (pH 8.0) containing 0.1 mM EDTA
- Thermal cycler (MJ Research)
- Agarose (Amersham Biosciences)
- Ethidium bromide (10 mg/ml) (Sigma)
- 1× TBE buffer (89 mM Tris; 89 mM boric acid; 2 mM EDTA)
- Electrophoresis apparatus
- Spectrophotometer

Method

1. Use 10 ng of genomic DNA as a template in a DOP-PCR mixture containing 1 µl of TaKaRa LA *Taq* polymerase, 50 µl of 2× GC buffer, 400 µM dNTPs, 4 µM DOP primer and nuclease-free water up to a final volume of 100 µl[b].
2. Perform DOP-PCR in a thermal cycler with an initial incubation of 93°C for 1 min[c], followed by eight cycles of 93°C for 1 min, 30°C for 1 min, and 72°C for 3 min (Stage 1)[d], and 28 cycles of 93°C for 1 min, 60°C for 1 min, and 72°C for 3 min (Stage 2)[e].
3. Run 5–10 µl of the DOP-PCR products including the negative control on a 1% agarose gel to assess fragment size and the success of the reaction[f].
4. Dilute the DOP-PCR products with four volumes of 10 mM Tris-HCl (pH 8.0) containing 0.1 mM EDTA and store at -20°C until use.

Notes

[a]The DOP-PCR method is as described previously (9) with slight modifications.
[b]It is important to include a negative control, which includes all of the reaction constituents with the exception of DNA.
[c]The initial denaturation for 8 min at 96°C, as suggested in (9), can be omitted with no effect on the efficiency of the DOP-PCR protocol, at least for the PCR targets tested in our work (11).
[d]Low-temperature annealing and extension, which occurs at several binding sites across the genome.
[e]Elevated annealing temperature, allowing more specific priming of the fragments tagged with the primer sequence.
[f]The negative control lane should not show any amplification. If it does, this suggests possible contamination and therefore reactions must be repeated. We would suggest using fresh reagents.

Protocol 3

Direct sequencing for SNP analysis

Equipment and Reagents

- AmpliTaq Gold DNA polymerase (5 units/μl) with the GeneAmp 10× PCR Gold Buffer (Applied Biosystems), or another comparable hot-start enzyme
- 500 nM PCR primers (Sigma Genosys)
- 25 mM $MgCl_2$ stock solution (Roche Diagnostics)
- 200 μM dNTP mix (Takara Bio)
- QIAquick PCR Purification Kit (Qiagen)
- Spectrophotometer
- BigDye Terminator Version 3.1 Cycle Sequencing Kit (Applied Biosystems)
- DNA sequencer (Applied Biosystems)
- Thermal cycler (MJ Research)
- SEQSCAPE Version 2.0 (Applied Biosystems)

Method

1. Prepare a 10 μl PCR mixture containing 1 μl of the diluted DOP-PCR product (approximately 10–15 ng of amplified DNA), 0.5 units of AmpliTaq Gold DNA polymerase, 200 μM dNTPs, 3.1 mM $MgCl_2$, and 500 nM of each primer.
2. PCR amplify using the following protocol: initial incubation at 95°C for 10 min; followed by 40 cycles of 95°C for 30 s, optimal annealing temperature for each primer pair[a] for 30 s, and 72°C for 1 min; and a final incubation at 72°C for 10 min.
3. Purify the PCR products using the QIAquick PCR Purification Kit, following the manufacturer's instructions.
4. Determine the yield of the PCR by measuring absorbance at 260 nm using a spectrophotometer.
5. Using the PCR products as templates, perform a cycle sequencing reaction using the BigDye Terminator Version 3.1 Kit according to the manufacturer's instructions[b].
6. Perform direct sequencing using a DNA sequencer and analyze the SNP types using SEQSCAPE Version 2.0 software[c].

Notes

[a]The primer pairs and optimal annealing temperatures used for these experiments are specific for the SNPs of interest and thus should be determined for each experiment.
[b]The quantity of PCR product used for sequencing varies depending on the size of the product. For 100–200 bp, use 1–3 ng of DNA; for 200–500 bp, use 3–10 ng of DNA; for 500–1000 bp, use 5–20 ng of DNA; for 1000–2000 bp, use 10–40 ng of DNA; for >2000 bp, use 20–50 ng of DNA (www.appliedbiosystems.com).
[c]Other instruments and software may also be used for the sequence analysis.

Protocol 4

High-throughput SNP typing[a]

Equipment and Reagents

- AmpliTaq DNA polymerase, Stoffel fragment (5 units/μl) with the 10× Stoffel buffer (Applied Biosystems)
- 20 nM TAMRA-labeled SSP-PCR primer (Sigma Genosys)
- 20 nM Cy5-labeled SSP-PCR primer (Sigma Genosys)
- 25 mM $MgCl_2$ stock solution (Roche Diagnostics)
- 200 μM dNTP mix (Takara Bio)
- 10 mM Tris-HCl (pH 8.0)
- 384-Well, hard-shell, thin-walled plates (MJ Research)
- 384-Well, glass-bottomed plates (Olympus Corporation)
- Single-molecule fluorescence detection (SMFD) system (Olympus Corporation)
- Thermal cycler (MJ Research)

Method

1. Using diluted DOP-PCR products as templates, perform PCR to amplify a fragment including an SNP site (see *Protocol 3*).
2. Perform SSP-PCR using the two competitive allele-specific primers in a 10 μl reaction containing 1× Stoffel buffer, 0.5 units of AmpliTaq DNA polymerase Stoffel fragment, 200 μM dNTPs, 2.5 mM $MgCl_2$, 20 nM of each primer, and 0.5 μl of the first PCR product as template.
3. PCR amplify in 384-well, hard-shell, thin-walled plates using the following protocol: initial incubation at 95°C for 2 min; followed by 40 cycles of ramping at 0.1°C/s to 95°C, 95°C for 30 s, optimal annealing temperature for each SNP for 30 s, and 72°C for 30 s; and a final incubation at 72°C for 10 min.
4. Transfer 4 μl of the SSP-PCR products into separate wells of a 384-well, glass-bottomed plate and dilute with 24 μl of 10 mM Tris-HCl (pH 8.0).
5. Analyze SNPs in the SSP-PCR products by FCS using the SMFD system[b]. Measure fluorescence at both 543 and 633 nm excitation wavelengths. Subject the mixture to FCS measurements and perform three 3 s measurements for each well.
6. Analyze the SNP genotypes using the software supplied with the SMFD system (examples of typing results are shown in *Fig. 2*).

Notes

[a]We perform both the first PCR and SSP-PCR in a thermal cycler capable of holding 384-well plates, as this enables us to perform high-throughput SNP analysis. Thermal cyclers capable of holding individual 0.2 or 0.5 ml tubes or 96-well plates are likely to be suitable.

[b]Other instruments and software may also be used for sequence analysis.

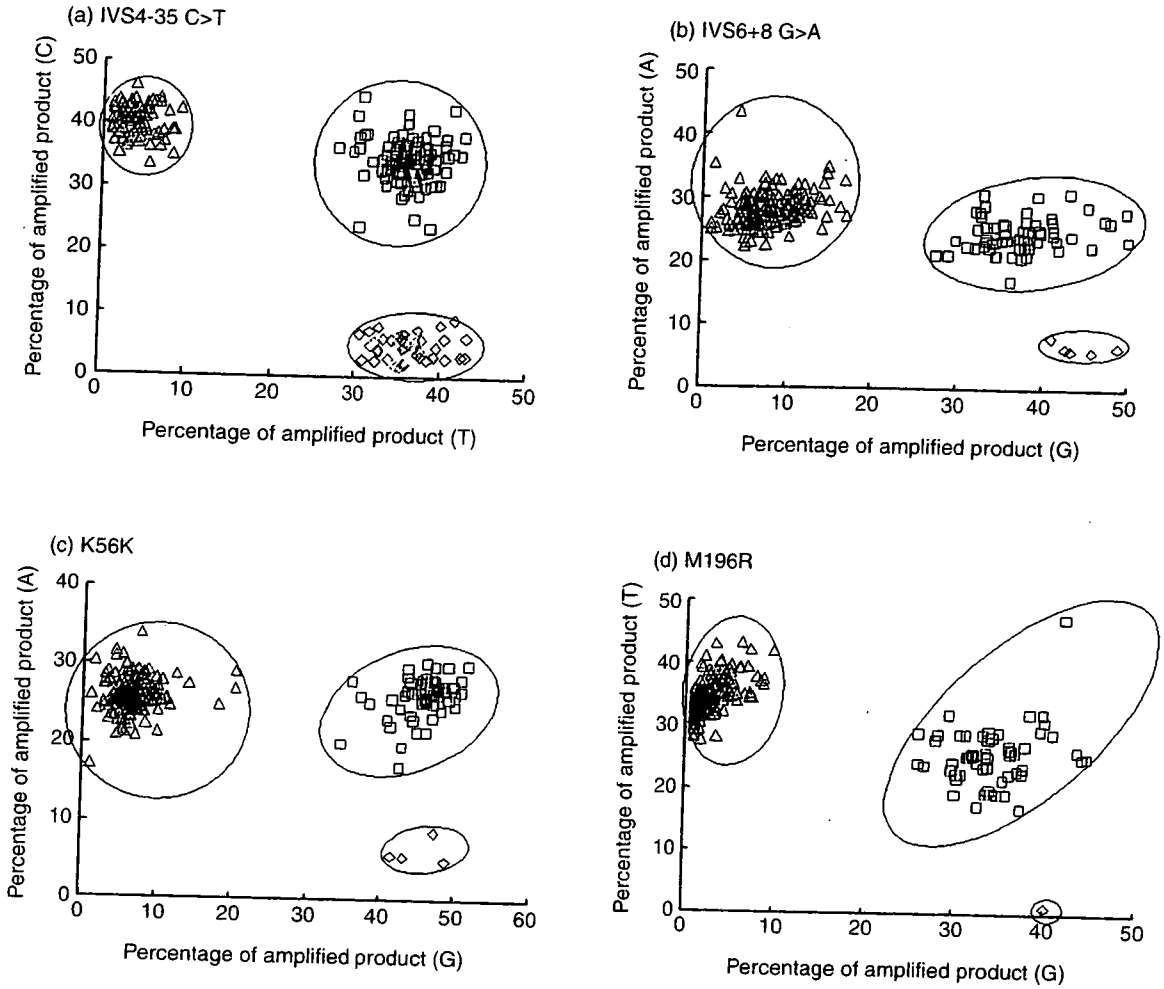

Figure 2. SNP typing results as determined by FCS using DOP-PCR products as templates. A total of 216 samples was analyzed. The genomic DNA concentration was measured precisely using the PicoGreen method, and 10 ng of genomic DNA was used as the template for a 100 µl DOP-PCR. One microlitre of fivefold-diluted product was used as the template for a subsequent PCR. Genotypes were determined by sequencing of the genomic DNAs. (*a*) TNFR1 IVS4-35 C>T: ◇, TT; □, TC; △, CC. (*b*) TNFR1 IVS6+8 G>A: ◇, GG; □, GA; △, AA. (*c*) TNFR2 K56K: ◇, GG; □, GA; △, AA. (*d*) TNFR2 M196R: ◇, GG; □, GT; △, TT. The *x*-axis shows the percentage of amplified product for 633 nm (Cy5), while the *y*-axis shows the percentage of amplified product for 543 nm (TAMRA).

3.1. Results

3.1.1. Genome coverage

Cheung & Nelson (9) showed by microsatellite genotyping that a large proportion of the genome can be amplified by DOP-PCR. In their study, all 55 microsatellites tested were efficiently amplified from the DOP-PCR products. Our experience of SNP analysis also indicates that most regions in the genome can be amplified by DOP-PCR. We have succeeded in PCR amplification of 431 out of 441 SNPs (98%) using DOP-PCR products as PCR templates. Telenius *et al.* (1) demonstrated that a single degenerate primer can efficiently amplify DNA from the genomes of non-human species, including mouse and *Drosophila*.

3.1.2. Starting template DNA

Precise measurement and normalization of the amount of template DNA is important. DOP-PCR is performed in a 100 µl reaction mixture using 10 ng of genomic DNA as starting template. A shortage of genomic DNA template sometimes leads to a lower reliability of genotyping for some SNPs. Thus, the PicoGreen method is used for precise measurement of the genomic DNA concentration. The concentration of genomic DNA is adjusted with 10 mM Tris-HCl (pH 8.0) containing 0.1 mM EDTA.

3.1.3. DOP-PCR yield

DOP-PCR can amplify genomic DNA more than 100-fold. Using 10 ng of genomic DNA as a template for DOP-PCR, 500 different PCRs are possible from the resulting WGA product (see *Figs. 2* and *3*). SNP typing sometimes failed when we used lower amounts of DOP-PCR products, indicating that further dilution of DOP-PCR products results in reduced reliability of genotyping for some SNPs. Cheung & Nelson (9) showed that 40 ng of genomic DNA was amplified with DOP-PCR to an average of 8 µg (200-fold amplification) as determined by A_{260}. In the same study, all microsatellite markers tested were amplified 200-600-fold from 0.6-40 ng of genomic DNA.

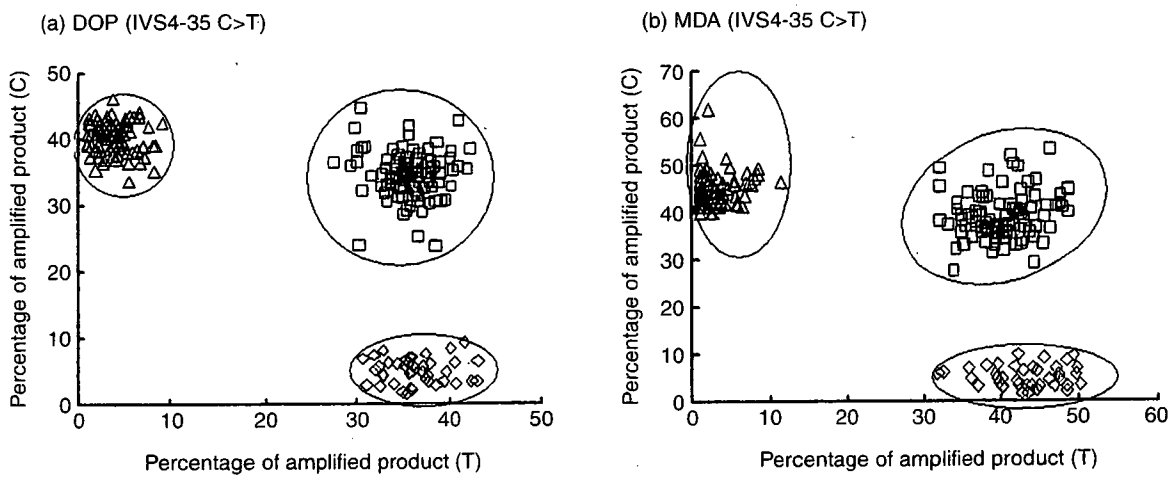

Figure 3. SNP typing results using DOP-PCR and MDA products as templates as determined by FCS (using precisely determined concentrations of genomic DNA).
SNP TNFR1 IVS4-35 C>T was analyzed in 216 samples. The genomic DNA concentration was measured precisely by the PicoGreen method. (*a*) Ten nanograms of genomic DNA was used as the template for a 100 µl DOP-PCR. One microlitre of fivefold-diluted product was used as the template for a subsequent PCR. (*b*) Ten nanograms of genomic DNA was used as the template for a 20 µl MDA reaction (using the GenomiPhi Kit, Amersham Biosciences, according to the manufacturer's instructions). One microlitre of 25-fold-diluted product was used as the template for a subsequent PCR. Genotypes were determined by sequencing of genomic DNAs. Samples are denoted by the corresponding genotype symbols as follows: ◇, TT; □, TC; △, CC. The *x*-axis shows the percentage of amplified product for 633 nm (Cy5), while the *y*-axis shows the percentage of amplified product for 543 nm (TAMRA).

3.1.4. DOP-PCR product size

The DOP-PCR products range from 200 to 1000 bp based on ethidium bromide staining of agarose gels (9). In our SNP typing studies, PCR primers were designed to produce amplification fragments up to 500 bp. Successful PCR amplifications using DOP-PCR products as template indicate that fragments of more than 500 bp in length can be obtained by DOP-PCR.

3.1.5. Amplification bias

Occasionally, we observe biased amplification of some heterozygous samples in mass SNP typing (see *Fig. 4a*, samples situated between clusters AA and CA, denoted by crosses). In this case, the amount of genomic DNA for some of the samples may not have been sufficient (see section 3.1.2). In addition, in microsatellite analysis, Grant *et al.* (10) noticed some preferential amplification of shorter alleles, although other reports have described equal amplification for microsatellites (9). It is important to take these points into consideration when using DOP-PCR-amplified DNA.

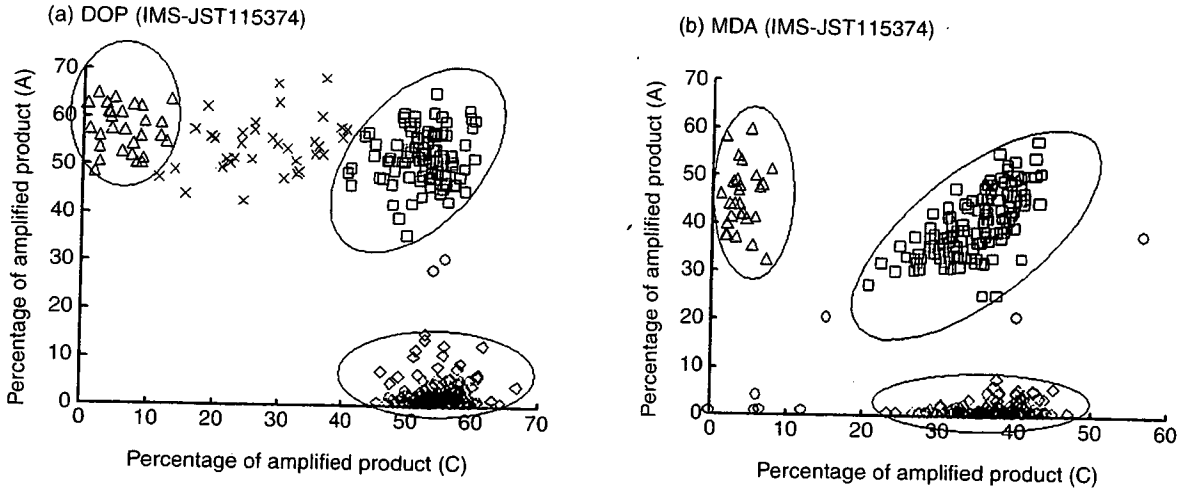

Figure 4. SNP typing results using DOP-PCR and MDA products as template as determined by FCS (using roughly measured concentrations of genomic DNA).
SNP IMS-JST115374 was analyzed in 246 samples. The genomic DNA concentration was roughly measured using a spectrophotometer. (*a*) Ten nanograms of genomic DNA was used as template for a 100 µl DOP-PCR. One microlitre of fivefold-diluted product was used as template for the subsequent PCR. (*b*) Ten nanograms of genomic DNA was used as template for a 20 µl MDA reaction (using the GenomiPhi Kit, Amersham Biosciences, according to the manufacturer's instructions). One microlitre of the 25-fold-diluted product was used as the template for the subsequent PCR. Samples are denoted by the corresponding genotype symbols as follows: ◇, CC; □, CA; △, AA; ○ and ×, not possible to judge. The *x*-axis shows the percentage of amplified product for 543 nm (TAMRA), while the *y*-axis shows the percentage of amplified product for 633 nm (Cy5).

3.1.6. Multiple-displacement amplification (MDA) provides greater accuracy in downstream genotyping assays

Recently, commercial kits (GenomiPhi, Amersham Biosciences; REPLI-g, Qiagen) employing MDA (see *Chapters 8–11*) have been used for WGA. When the amount of genomic DNA is sufficient (10 ng) for all samples, SNP typing using DOP-PCR products as template provides accurate results (see *Fig. 2*), comparable to those obtained using MDA products (see *Fig. 3*). However, we occasionally observed cases where MDA-generated DNA gave greater genotyping accuracy in mass SNP typing than DOP-PCR-generated DNA (see *Fig. 4*). In such cases, it is possible that suboptimal amounts of DNA are present in the DOP-PCR-amplified sample. When we compared DOP-PCR and MDA-amplified DNA for SNP typing, we succeeded in typing 82.1% (348 of 424) and 95.8% (68 out of 71) of the SNPs, respectively, when using the same genomic DNA template for WGA. For example, in *Fig. 4*, 34 out of 36 samples situated between clusters AA and CA (indicated by crosses) by DOP-PCR (see *Fig. 4a*) were classified in the CA cluster by MDA (see *Fig. 4b*).

3.2. Conclusion

SNP typing can be successfully performed using DOP-PCR-amplified DNA. However, it is important to ensure that sufficient starting template is used in the DOP-PCR and that an appropriate amount of DOP-PCR product is used for any subsequent PCRs. The genotypes determined by SSP-PCR and FCS using DOP-PCR samples were 100% in agreement with those determined by direct sequencing of genomic samples. Under these conditions, for most if not all cases, there should be no or very little biased amplification by DOP-PCR.

4. REFERENCES

★★★ 1. **Telenius H, Carter NP, Bebb CE, Nordenskjold M, Ponder BA & Tunnacliffe A** (1992) *Genomics*, **13**, 718–725. – *First report of DOP-PCR.*

2. **Dietmaier W, Hartmann A, Wallinger S, *et al.*** (1999) *Am. J. Pathol.* **154**, 83–95.

3. **Hirose Y, Aldape K, Takahashi M, Berger MS & Feuerstein BG** (2001) *J. Mol. Diagn.* **3**, 62–67.

4. **Huang Q, Schantz SP, Rao PH, Mo J, McCormick SA & Chaganti RS** (2000) *Genes Chromosomes Cancer*, **28**, 395–403.

5. **Kittler R, Stoneking M & Kayser M** (2002) *Anal. Biochem.* **300**, 237–244.

6. **Telenius H, Pelmear AH, Tunnacliffe A, *et al.*** (1992) *Genes Chromosomes Cancer*, **4**, 257–263.

7. **Umayahara K, Numa F, Suehiro Y, *et al.*** (2002) *Genes Chromosomes Cancer*, **33**, 98–102.

8. **Kallioniemi A, Kallioniemi OP, Sudar D, *et al.*** (1992) *Science*, **258**, 818–821.

★ 9. **Cheung VG & Nelson SF** (1996) *Proc. Natl. Acad. Sci. U. S. A.* **93**, 14676–14679. – *The use of DOP-PCR-amplified DNA in SNP genotyping.*

10. **Grant SF, Steinlicht S, Nentwich U, Kern R, Burwinkel B & Tolle R** (2002) *Nucleic Acids Res.* **30**, e125.

11. **Bannai M, Higuchi K, Akesaka T, *et al.*** (2004) *Anal. Biochem.* **327**, 215–221.

12. **Jordan B, Charest A, Dowd JF, *et al.*** (2002) *Proc. Natl. Acad. Sci. U. S. A.* **99**, 2942–2947.

Available online at www.sciencedirect.com
SCIENCE DIRECT®
Analytical Biochemistry 346 (2005) 281–288
ANALYTICAL BIOCHEMISTRY
www.elsevier.com/locate/yabio

DigiTag assay for multiplex single nucleotide polymorphism typing with high success rate

Nao Nishida [a,b,*], Tetsuya Tanabe [c], Kento Hashido [b], Kouyuki Hirayasu [a], Miwa Takasu [a], Akira Suyama [d], Katsushi Tokunaga [a]

[a] *Department of Human Genetics, Graduate School of Medicine, The University of Tokyo, 7-3-1 Hongo, Bunkyo-ku, Tokyo 113-0033, Japan*
[b] *Biomedical Business Incubation Division, Olympus Corp., 2-3 Kuboyama-cho, Hachioji, Tokyo 192-8512, Japan*
[c] *R&D Division, NovusGene Inc., 2-3 Kuboyama-cho, Hachioji, Tokyo 192-8512, Japan*
[d] *Department of Life Sciences, Graduate School of Arts and Sciences, The University of Tokyo, 3-8-1 Komaba, Meguro-ku, Tokyo 153-8902, Japan*

Received 29 June 2005
Available online 31 August 2005

Abstract

As a consequence of Human Genome Project and single nucleotide polymorphism (SNP) discovery projects, several millions of SNPs, which include possible susceptibility SNPs for multifactorial diseases, have been revealed. Accordingly, there has been a strong drive to perform the investigation with all candidate SNPs for a certain disease without decreasing the number of analyzed SNPs. We developed DigiTag assay, which uses well-designed oligonucleotides called DNA coded numbers (DCNs) in multiplex SNP genotype analysis. During the analysis, the information of a genotype is converted to one of the DCNs in a one to one manner using oligonucleotide ligation assay (encoding). After the encoding reaction, only the DCNs regions and not the SNP specific regions are amplified using the universal primers and then SNP genotype is read out using DNA capillary arrays. DigiTag assay was found to be successful in SNP genotyping, giving a high success rate (24 of 27 SNPs) for randomly chosen SNPs. Moreover, this assay has the potential to analyze almost all kinds of the target SNPs by applying mismatch-induced probes and redesigned primer pairs at a low-cost.

Keywords: Genotyping method; Multiplex genotyping; SNPs; Mutation; Oligonucleotide ligation assay

Numerous single nucleotide polymorphisms (SNPs)[1] are considered to be candidate susceptibility or resistance genetic factors for multifactorial diseases such as hypertension, diabetes, and rheumatic diseases [1–5]. Large-scale case–control analyses of SNPs in candidate genes have revealed associations between various diseases and SNPs with the highest detection power [6–8]. Moreover, genome-wide association studies using SNPs have become important in the search for susceptibility and/or resistance genes [9,10]. Accordingly, large-scale whole-genome genotyping projects need high-throughput, cost-effective, and highly reliable technology to identify primary genes or SNPs. At present, there are a variety of SNP genotyping applications including microarray technology [11], molecular inversion probe genotyping [12], BeadArray genotyping technology (Illumina), 5′ exonuclease fluorescence-based assay (TaqMan) [13], pyrosequencing [14], single-base extension [15], matrix-assisted laser desorption/ionization time-of-flight mass spectrometry [16,17], and SNPlex (Applied Biosystems). However, many applications need to select relevant SNPs for their assay by in silico assay design, and then a portion of candidate SNPs will be excluded from investigation. To accomplish successful typing for all candidate SNPs at a low-cost, new technologies must be developed. In this study, we developed a new multiplex SNP typing method, named DigiTag assay, and performed typing for 28 SNPs using 40 genomic DNA samples. This approach

* Corresponding author. Fax: +81 3 5802 8619.
E-mail address: nishida-75@umin.ac.jp (N. Nishida).

[1] *Abbreviations used:* SNPs, single nucleotide polymorphisms; DCNs, DNA coded numbers; DTT, dithiothrecitol; SSC, standard saline citrate.

0003-2697/$ - see front matter © 2005 Elsevier Inc. All rights reserved.
doi:10.1016/j.ab.2005.08.007

uses well-designed oligonucleotides called DNA coded numbers (DCNs), which enable performance of multiplex SNP genotyping with high accuracy and reproducibility.

Materials and methods

DNA samples

Genomic DNA samples from 40 unrelated healthy donors were obtained from the Japan Health Science Foundation (Osaka, Japan). All donors provided written informed consent and samples were anonymized. One hundred nanograms of purified genomic DNA was dissolved in 20 μl TE buffer, pH 8.0 (Wako, Osaka, Japan), for use and stored at 4 °C.

Preparation of DNA coded numbers

DCNs were designed to be 69-mer oligonucleotides (Fig. 1). DCNs consist of three parts, designated SD (start-digit), D1 (first-digit), and ED (end-digit). SD and ED are the common DNA sequences prepared at both edges in all DCNs and are used for priming sites in the labeling step. D1s are different DNA sequences among DCNs and are used to identify SNPs of interest. We prepared two EDs (ED-1 and ED-2) for two alleles at each SNP. The sequences of the three DCN components have the same length of 23-mer and the uniform melting temperature of 60.5 ± 0.9 °C. The assignment of DCNs to the SNPs analyzed in this study is listed in the Supplementary Table.

We designed DCNs (i) to have a uniform melting temperature and length, (ii) to ensure specific hybridization only to complementary DCNs, (iii) to minimize interaction with other DCNs, and (iv) to prevent the formation of secondary structures [18,19]. Therefore, all DCNs can be uniformly amplified in a multiplex manner using the common priming sites (SD, ED-1, and ED-2). Furthermore, we can perform precise hybridization on the DNA capillary array using a set of DCNs with high reproducibility.

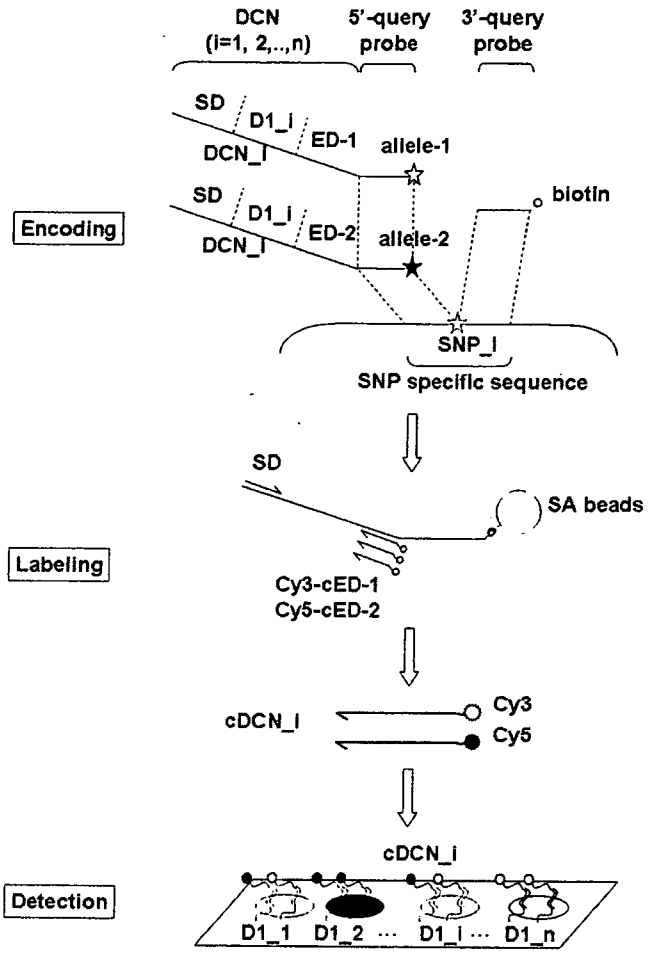

Fig. 1. Schematic representation of DigiTag assay. This assay has four steps to accomplish SNP typing: target preparation, encoding, labeling, and detection. DCNs are composed of three parts: SD, D1, and ED. SD and ED are the common DNA sequences prepared at both edges in all DCNs and are used for priming sites in the labeling step. Two EDs (ED-1 and ED-2) are prepared for two alleles at each SNP. D1s are different DNA sequences among DCNs and are used to identify SNPs of interest. DCN_i includes the common priming sites (SD, ED-1, and ED-2) and variable sequence (D1_i). Reverse complement sequences are written by attaching the character c before the sequence name.

Multiplex PCR from sample DNA

We designed multiplex PCR primers for each of the 28 SNP sites to have relatively long-length (average length 40-mer) and to give PCR product lengths of between 200 and 800 bp (average PCR product length 464 bp). To avoid spurious amplification products, we performed multiplex PCR by a two-step protocol (denature and extension steps) with elongated extension step for 6 min using specifically designed primer pairs.

Multiplex PCR was performed with 2.5 μl of genomic DNA and 1.25 pmol of primer pairs for 28 SNP sites in 50 μl of Multiplex PCR buffer, 0.2 μM dNTPs, and HotStarTaq DNA polymerase (Qiagen Multiplex PCR Kit, Qiagen, CA, USA). Cycling was performed as follows: 95 °C for 15 min, followed by 40 cycles of 95 °C for 30 s and 68 °C for 6 min. When necessary, the fragment length of 28 PCR products was confirmed by capillary electrophoresis (Agilent 2100 Bioanalyzer, Agilent, CA, USA) to evaluate the PCR efficiency.

Encoding reaction

We prepared two 5′-query probes and one 3′-query probe for a single SNP site (Fig. 1). The 5′-query probes have the sequence complementary to that of the 5′ flanking of the target SNP (average length 20-mer) and each of the probes has an allele-specific sequence. Two types of DCNs, which have ED-1 and ED-2, were attached to each of the 5′-query probes. The 3′-query probe has the sequence complementary to that of the 3′ flanking of the target SNP (average length 20-mer) and has a phosphate group on its 5′ end and a biotin molecule on its 3′ end.

Two microliters of multiplex PCR product was mixed in 30 μl of 20 mM Tris–HCl, pH 7.6, 25 mM potassium acetate, 10 mM magnesium acetate, 10 mM DTT, 1 mM NAD, 0.1% Triton X-100 (*Taq* DNA ligase buffer, New England BioLabs, MA, USA) with 10 fmol of each probe (56 5′-query and 28 3′-query probes), 0.1 μl of control mix, and 20 U *Taq* DNA ligase. The control mix was prepared to assess each step of this assay including (i) 10 fmol of control target oligonucleotides and 10 fmol of two 5′-query probes and one 3′-query probe (assigned to DCN_29) for positive control of entire step, (ii) 0.1 fmol of 3′ end biotinylated DCN_30 for positive control of washing step with streptavidin-coupled magnetic beads, and (iii) 10 fmol of nonlabeled DCN_31 for negative control of washing step with streptavidin-coupled magnetic beads. All components of the encoding reaction were mixed on ice. The encoding reaction was first held at 95 °C for 5 min, followed by 58 °C for 15 min. The reaction was stopped by holding temperature at 10 °C.

Labeling of DCNs

The ligated products were washed with 1 × binding and washing buffer (1 M NaCl, TE, pH 8.0) twice at room temperature after binding to streptavidin-coupled magnetic beads (Dynabeads M-280 streptavidin, Dynal, Oslo, Norway), following the manufacturer's protocol. Alkali denaturation was performed to remove the multiplex PCR product and then asymmetric PCR was performed with single-strands of the ligated products binding to streptavidin-coupled magnetic beads, 1.0 pmol of SD, 10.0 pmol of Cy3-labeled reverse complement of ED-1 (Cy3-cED-1), 10.0 pmol of Cy5-labeled reverse complement of ED-2 (Cy5-cED-2), 2.5 U of *Ex Taq* polymerase in a 20 μl of 20 mM Tris–HCl, pH 8.0, 100 mM KCl, 0.1 mM EDTA, 1 mM DTT, 0.5% Tween 20, 0.5% Nonidet P-40, 50% glycerol, 2 mM each dNTP (*Ex Taq* Buffer, TaKaRa, Shiga, Japan). Asymmetric PCR was first held at 95 °C for 1 min, followed by 20 cycles of 95 °C for 30 s, 55 °C for 30 s, and 72 °C for 30 s.

Hybridization and detection on DNA capillary array

The DNA capillary array is a DNA detection device integrating oligonucleotide probes attached to specific locations in eight-parallel capillaries on a slide glass (see Fig. 3B, Olympus, Tokyo, Japan). Thirty-two types of oligonucleotide probes (28 probes for 28 SNPs and 4 probes for validation controls of the assay) identical to D1 sequences of DCNs were immobilized in each capillary. The ready-to-use DNA capillary arrays were stored in a desiccator at room temperature until use.

A hybridization mixture was prepared by mixing the supernatant of asymmetric PCR mixture in 24 μl of hybridization buffer containing 0.5 × SSC, 0.1% SDS, 15% formamide, 1 mM EDTA, with 2 μl of hybridization control. The hybridization control for ensuring the hybridization step was prepared with 5 fmol of Cy3-labeled D1_32 and Cy5-labeled D1_32. Twenty microliters of the hybridization mixture was applied to each capillary on the DNA capillary array. Hybridization was carried out for 30 min at 37 °C in a hybridization oven. After hybridization, the glass slides were washed in a washing buffer (0.1 × SSC, 0.1% SDS) by shaking at 60 rpm for 5 min. The glass slides were consecutively washed in distilled water by shaking at 60 rpm for 1 min and then dried by centrifugation at 2000 rpm for 1 min. Hybridization images were scanned at photomultiplier voltages of 400 V for Cy3 and 520 V for Cy5 using a commercially available DNA chip scanner and fluorescence image analysis was performed using commercially available software (GenePix 4000B unit and GenePix Pro 4.1 software package, Axon Instruments, CA, USA).

Results

Schematic representation of DigiTag assay

This assay is performed in four steps: target preparation, encoding, labeling, and detection (Fig. 1). In this assay, multiplex PCR is performed with genomic DNA to prepare target fragments before the encoding step. For multiplex PCR, we designed the primer pairs to have 40-mer in average length and performed multiplex PCR by a two-step protocol (denature and extension steps) with elongated extension step for 6 min. The long-length primers and elongated extension step are essential for multiplex PCR to uniformly amplify all of the target fragments. In the encoding step, the 5′-query probe and 3′-query probe are successfully concatenated by *Taq* DNA ligase when two probes are fully complementary to adjacent regions on the target fragment [20]. The information of genotype is converted to one of the DCNs by a one to one manner in the encoding step. After the encoding step, single-strand forms of alkali denatured ligation products serve as templates in asymmetric PCR using Cy3- and Cy5-labeled primer pairs (SD, Cy3-cED-1, and Cy5-cED-2). The Cy3- and Cy5-labeled PCR products are gathered as single-strand forms of complementary DCNs and are then hybridized with the D1 probes on the DNA capillary array to reveal SNP genotypes by reading the signals from the various D1s. If the genomic DNA sample is homozygous for a certain SNP, a single color signal from Cy3 or Cy5 is detected from the corresponding spot on the DNA capillary array. In contrast, both signals are present when the sample is heterozygous.

Optimization of reaction condition in encoding step and DCN amplification rate

We first investigated the ligation conditions in the encoding step using a SNP located in the *PLOD* gene on human chromosome 1p36 as a model SNP (JSNP ID IMSJST068774). We prepared four types of 5′-query probes with four types of DCNs, each of which had one of the original SNP bases G and C and the two artificial SNP bases A

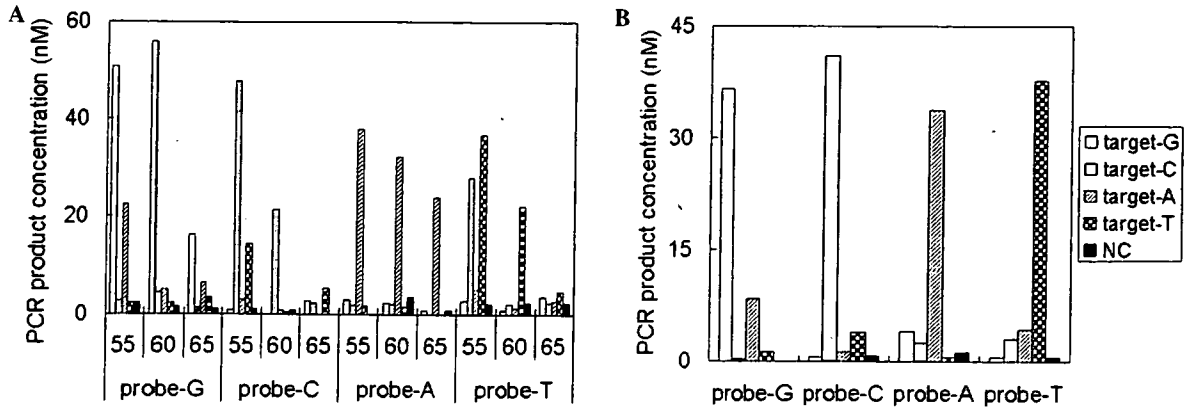

Fig. 2. Encoding rates of four SNP bases at different ligation temperatures. Encoding rate was compared as the amount of PCR product in the combination with four types of 5′-query probes and four types of target oligonucleotides. NC means that no target was included in the encoding reaction. Average amount of PCR product was calculated from three independent experiments. (A) The ligation reaction was performed at three temperatures: 55, 60, and 65 °C for 15 min. (B) The ligation reaction was performed at 58 °C for 15 min.

and T (see Supplementary Table). To investigate the encoding conditions, we prepared four types of 30-base target oligonucleotides identical to the SNP specific sequences. The encoding conditions were investigated by varying the ligation temperature from 55 to 65 °C (Fig. 2A). The encoding rate was compared as the amount of PCR products after performing 25 cycles of PCR with SD and reverse complement of ED (cED) primers using the ligated products as templates. When the ligation reaction was performed at 58 °C for 15 min, the signal intensities from perfect-match pair of 5′-query probe and target oligonucleotide were substantially higher than those from non-perfect-match pairs (Fig. 2B). False-positive signals were also suppressed at this ligation condition among the four SNP bases. False-positive signals increased at lower ligation temperatures, particularly when G-T mismatch occurred between 5′-query probe and target oligonucleotide. The intensities of positive signals decreased with ligation temperatures above 58 °C. Moreover, it became clear that the SNP base should be located at the 3′ end of the 5′-query probes to ensure precise discrimination between alleles (data not shown). When the SNP base was located at the 5′ end of the 3′-query probe, false-positive signals were significantly high and therefore resulted in incorrect genotyping.

PCR amplification rate was investigated by real-time PCR among DCNs used in multiplex SNP typing. A single DCN was added to a separate tube in 10-fold dilutions between 100 and 1 pM. PCR amplification rates of each DCN were calculated based on the results of real-time PCR. As expected, PCR amplification rate was found to be uniform at about 1.8 at concentrations between 100 and 1 pM (data not shown).

Multiplex typing for 28 SNPs using 40 genomic DNA samples

We then randomly selected 28 SNPs from a 500-kb region including the *IL-4* and *IL-13* genes on human chromosome 5q31-33, which contains several candidate genes related to immune disorders. We subsequently designed probes for the 28 SNP sites to give properties similar to those for *PLOD* SNP to obtain similar ligation efficiency among the 28 SNP sites to be analyzed in a single tube. The 5′-query probes and 3′-query probes were designed to have the uniform melting temperatures, 52.9 ± 1.8 and 55.0 ± 1.4 °C, respectively. The SNP genotypes of 40 genomic DNA samples were alternatively determined by direct sequencing and were used as reference data.

Multiplex PCR products including the 28 SNP sites showed similar band patterns with different individual DNA samples, although it was difficult to clearly discern all 28 PCR products due to the limitation of the electrophoretic resolution (Fig. 3A). Multiplex SNP typing for 28 SNPs was then performed using the multiplex PCR products as targets. The DNA capillary array demonstrated hybridization images of each sample in each capillary having 32 spots (28 probes for 28 SNPs and 4 probes for validation controls, see Fig. 3B). The hybridization image was analyzed using a DNA chip scanner, and the Cy3 and Cy5 signal intensities of each spot were plotted to produce a scatter diagram (Fig. 3C). The SNP 13 was monomorphic in 40 genomic DNA samples and was excluded from further analysis. For 24 SNPs (except for SNP 6, SNP 9, and SNP 19), three distinct clusters corresponding to two homozygous and one heterozygous genotypes were observed, although the average signal intensity for the 24 SNP sites fluctuated between 100 and 16,000. The fluctuated intensities presumably result from different efficiencies of PCR in the target preparation step by the multiplex PCR.

Indistinct clusters were observed for SNP 6, SNP 9, and SNP 19. For SNP 6 and SNP 9, the false-positive signals were detected when we performed singleplex SNP typing using target oligonucleotides identical to the SNP specific sequences (Figs. 4A and B). To suppress the false-positive signals observed from SNP 6 and SNP 9, we prepared

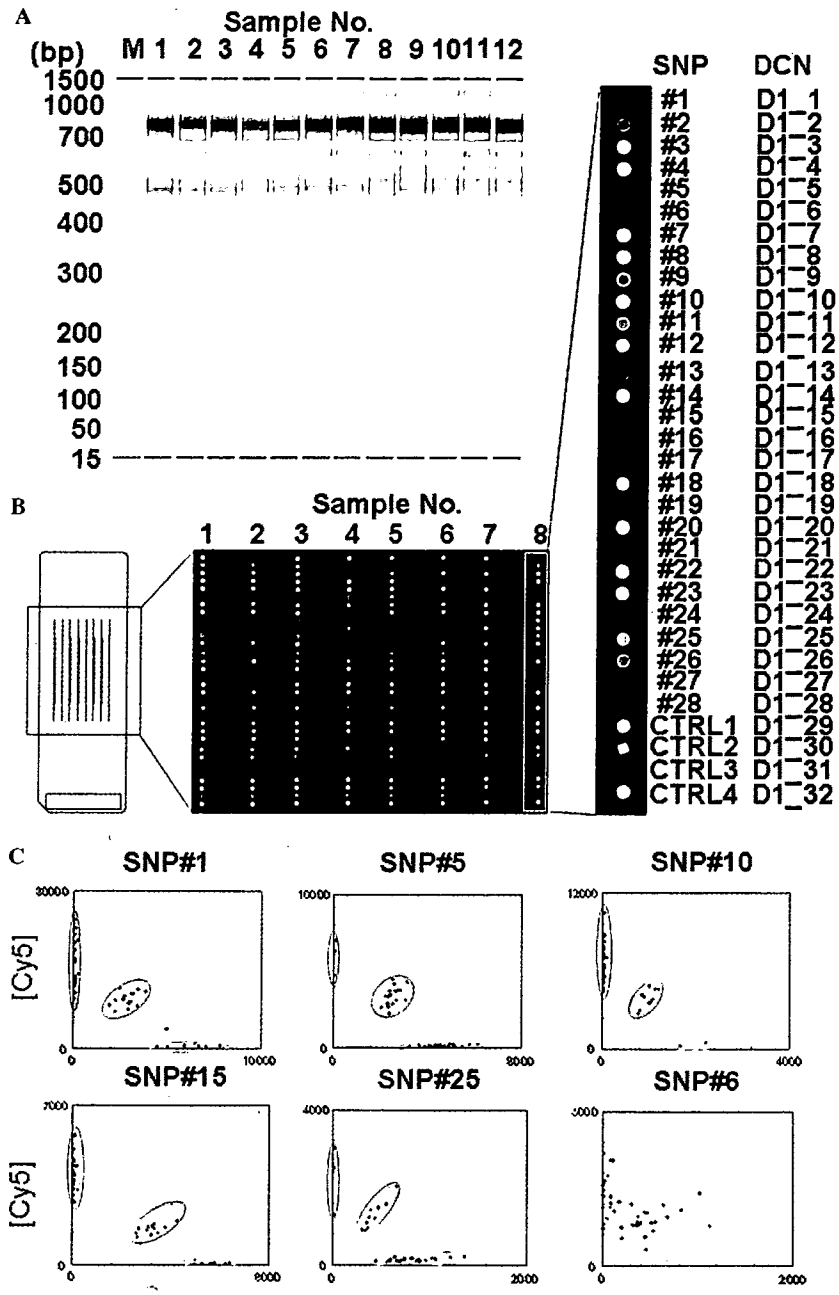

Fig. 3. Multiplex SNP typing for 28 SNPs using 40 genomic DNA samples. (A) Gel images of multiplex PCR products with different individual samples. In all sample lanes, the sample bands were observed between two inner markers; 15 and 1500 bp. (B) Hybridization images of the DNA capillary array. (C) Scatter diagrams for randomly chosen 6 SNPs from 28 SNPs.

three types of mismatch-induced 5′-query probes, which had an artificial mismatch at the fourth position from the SNP base. The encoding rate was investigated using mismatch-induced 5′-query probes and target oligonucleotides identical to the SNP specific sequences by comparing the amount of PCR products after performing 25 cycles of PCR using the ligated products as templates. All of the three mismatch-induced 5′-query probes can effectively suppress the false-positive signals without diminishing the positive signals from the perfect-match pair of the mismatch-induced 5′-query probe and target oligonucleotide (Figs. 4A and B). We then performed multiplex typing using one of the mismatch-induced 5′-query probes for each of two SNPs. Scatter diagrams showed that three clusters from perfect-match 5′-query probes were indistinctively observed (Figs. 4C and D) as compared to the mismatch-induced 5′-query probes (Figs. 4E and F). For SNP 19, many samples did not belong to any clusters, presumably due to insufficient amplification of the target fragment in multiplex PCR.

In 24 successfully genotyped 24 SNPs, 8 miscallings were observed among 960 genotypes. The percentage of calling rate (number of identified SNPs divided by the total number examined) was 99.2% and the concordance rate with